THE JOURNAL OF PHYSICAL CHEMISTRY B
A JOURNAL OF THE AMERICAN CHEMICAL SOCIETY

pubs.acs.org/JPCB

Perspective

A Brief Guide to the Structure of High-Temperature Molten Salts and Key Aspects Making Them Different from Their Low-Temperature Relatives, the Ionic Liquids

Shobha Sharma, Alexander S. Ivanov,* and Claudio J. Margulis*

Cite This: *J. Phys. Chem. B* 2021, 125, 6359–6372

Read Online

ACCESS | Metrics & More | Article Recommendations

ABSTRACT: High-temperature molten salt research is undergoing somewhat of a renaissance these days due to the apparent advantage of these systems in areas related to clean and sustainable energy harvesting and transfer. In many ways, this is a mature field with decades if not already a century of outstanding work devoted to it. Yet, much of this work was done with pioneering experimental and computational setups that lack the current day capabilities of synchrotrons and high-performance-computing systems resulting in deeply entrenched results in the literature that when carefully inspected may require revision. Yet, in other cases, access to isotopically substituted ions make those pioneering studies very unique and prohibitively expensive to carry out nowadays. There are many review articles on molten salts, some of them cited in this perspective, that are simply outstanding and we dare not try to outdo those. Instead, having worked for almost a couple of decades already on their low-temperature relatives, the ionic liquids, this is the perspective article that some of the authors would have wanted to read when embarking on their research journey on high-temperature molten salts. We hope that this will serve as a simple guide to those expanding from research on ionic liquids to molten salts and *vice versa*, particularly, when looking into their bulk structural features. The article does not aim at being comprehensive but instead focuses on selected topics such as short- and intermediate-range order, the constraints on force field requirements, and other details that make the high- and low-temperature ionic melts in some ways similar but in others diametrically opposite.

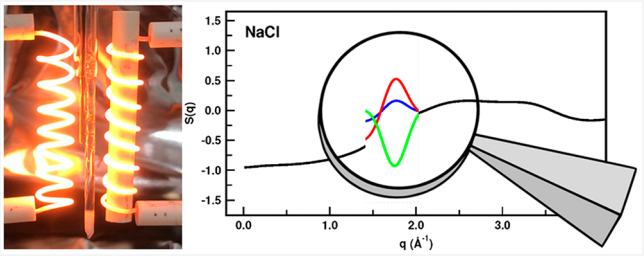

INTRODUCTION

There has been a constant stream of articles[1−69] including salts in their molten or glass states since the early 1900s; see for example, the works of Zachariasen[70] and Rosenhain.[71] Yet, through the years, molten salts continue to be rediscovered for applications in energy technologies including nuclear energy,[72−76] solar energy harvesting,[77−79] batteries,[80−82] and separations[83] to mention just a few. The 1970s and early 1980s brought a series of interesting spectroscopic measurements that could be directly linked to the 3D structure of salts in the molten phase, in particular via Raman spectroscopy,[16−18,22,23,29] and soon after, pioneering X-ray and neutron scattering results[30,31,33−36,38,43] revealed more information about short and intermediate range order. These results followed or were followed by pioneering theory developments and early simulation work.[11−13,15,19−21,24−28,32,37,39,41,42,44−52,59] Multiple force fields to simulate salts have been developed, but modern point-polarizable force fields with quantum mechanical accuracy[53−58,61] are the current go-to models for most simulations of divalent and multivalent cationic systems coupled with polarizable anions. Recently, a faster Drude-type model that includes some of the same ingredients as in these other more expensive models has also been successfully developed and applied to the case of $MgCl_2$ and its mixtures with KCl.[84] A variety of articles based on machine-learning simulation schemes for molten salts have also recently appeared in the literature.[85−90] Advances in computational models have come hand-in-hand with new experimental studies,[40,59,60,62−69,91−94] and in some cases, the combination of these challenges strongly entrenched assumptions, for example the octahedral coordination of U^{3+},[94] the tetrahedrality in coordination for Mg^{2+},[58,95] and other properties that collectively have influenced the literature for 30 years or more.[58,93−96] The works cited thus far are meant to provide some context and are not exhaustive or cover many of the most

Received: February 4, 2021
Revised: April 8, 2021
Published: May 28, 2021

https://doi.org/10.1021/acs.jpcb.1c01065
J. Phys. Chem. B 2021, 125, 6359−6372

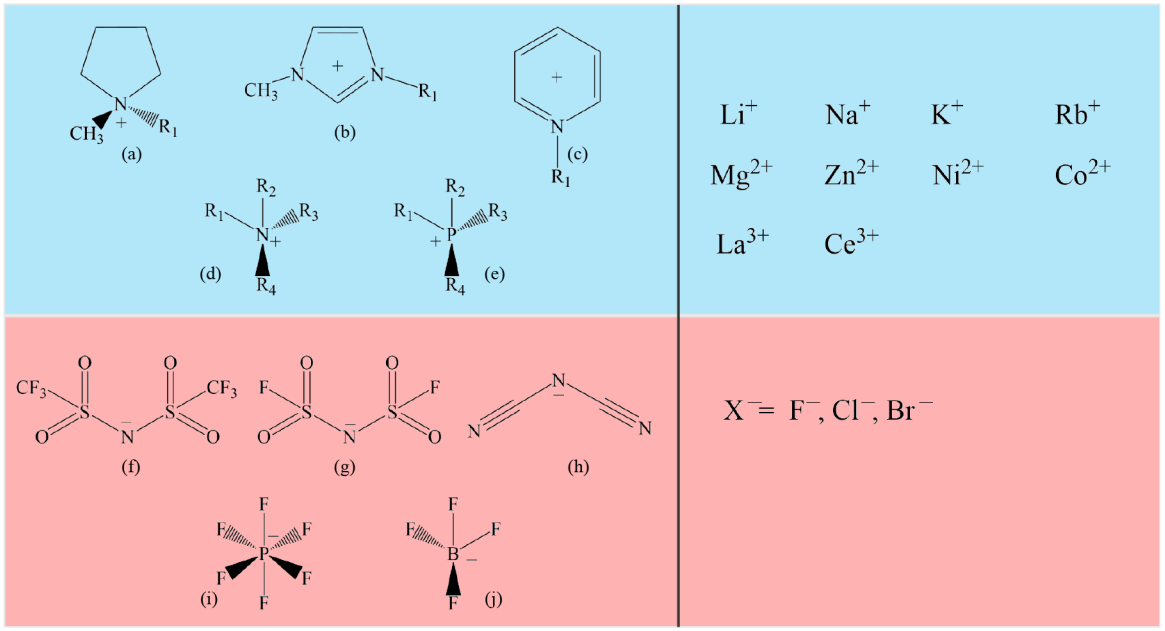

Figure 1. (Left) some common ions or ion families associated in the literature with ionic liquids and (right) typical ions associated with high-temperature molten salts.

studied salts and their mixtures of which the eutectics are of special relevance.

Literature on ionic liquids (ILs) also dates to the early 1900s with the work by Walden[97] on ethylamonium nitrate, and a few decades later to work on chloroaluminates.[98] The reader is encouraged to read the authoritative history of ionic liquids recently published by Welton and references therein.[99] For the purpose of this perspective article, when comparisons are made between molten salts and ILs (see Figure 1), these are made with the most common modern ILs in mind, which are based on organic cations and organic or inorganic anions instead of the early chloroaluminates.

RESULTS AND DISCUSSION

Before we embark into a detailed discussion about X-ray and neutron scattering, including the temperature dependence of the features in the structure factor, it is worth highlighting some experimental and computational peculiarities associated with these systems that will be useful to those coming from more conventional condensed phase liquid systems.

Experimental Caveats and Considerations. Over the past decades, advancements in high-energy X-ray and enhanced flux neutron diffraction techniques have provided opportunities to obtain the structure function for liquid salts out to large momentum transfers (q), leading in principle to high-resolution pair distribution functions that can be directly compared to simulation results and thus are important as a benchmark for the development of accurate atomistic models. Confidence in such models is important for the prediction of transport and thermodynamic properties, as some of these are challenging to measure for salts at high temperature. An example is ionic diffusivity, which is readily accessible for ILs via NMR measurements but less so for molten salts. The principles of X-ray/neutron diffraction theory and the details of total scattering data processing are extensively discussed elsewhere[100−104] and need not be elaborated here, except perhaps to mention that notation and nomenclature in the literature have taken slightly different forms for molten salts and ILs. In fact, even within the molten salts literature, there is significant variation in the use of variables; an excellent resource to start understanding these is a comprehensive review by Keen.[105]

Total X-ray and neutron scattering measurements are not without some experimental uncertainty stemming from a number of challenges posed not only by the chemistry of the particular salt but also by the extreme conditions under which such measurements are carried out. In order to obtain reliable X-ray or neutron scattering data, one needs first to make sure that samples are of high quality and their compositions accurately known. Due to the hygroscopic nature of ILs and molten salts, this constitutes a challenge. Whereas the problem is well understood and relatively easy to control in the case of ILs, it is significantly more challenging for molten salts where the quick uptake of atmospheric water for some very hygroscopic salts may cause noticeable changes in sample composition, leading to uncertainties in experimental data reduction and analysis. Some inorganic salt hydrates readily undergo hydrolysis upon a temperature increase, resulting in a variety of unanticipated chemical species such as metal oxides.[106] Therefore, moisture-sensitive samples are usually prepared in an inert atmosphere glovebox and loaded into 1−2 mm quartz capillaries. While IL samples are usually sealed with a silicon rubber or wax to prevent water absorption, inorganic salt samples need to be flame-sealed to enable X-ray/neutron diffraction data collection at high-temperature regimes (see Figure 2). In addition, when compared with ILs, a more complex measurement setup is needed for molten salts where the quartz tube is placed in a furnace sample holder consisting of two resistive heaters as shown in Figure 3. Note, however, that quartz is by no means the universal containment material for all possible salts or salt mixtures, since for example fluorides tend to react with glass at elevated temperatures, requiring the utilization of Pt−Rh[107] or boron nitride containers in the case of X-ray scattering measurements.

In addition to the described chemical and technical complexities, there is also the fact that the structure function

https://doi.org/10.1021/acs.jpcb.1c01065
J. Phys. Chem. B 2021, 125, 6359−6372

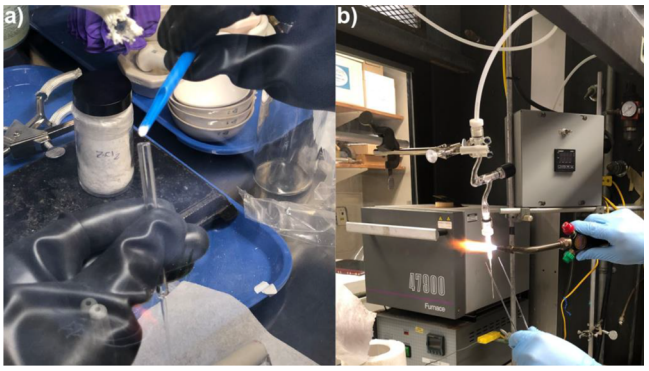

Figure 2. (a) Loading the salt sample in a glovebox. (b) Sealing the sample in a capillary.

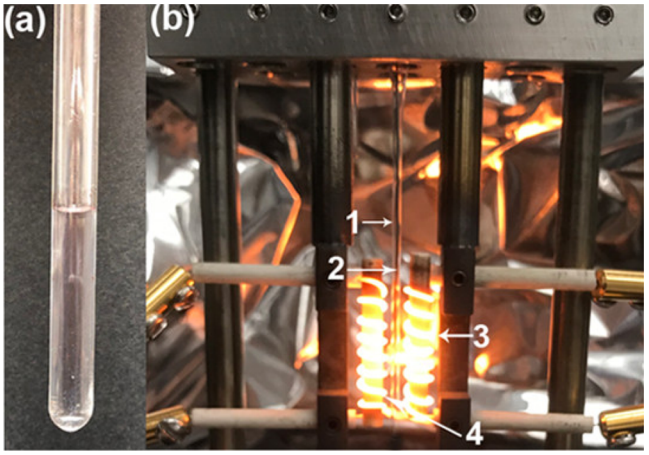

Figure 3. (a) Inorganic molten salt mixture ($MgCl_2$/KCl) at 1073 K. (b) Experimental setup typically used for high-energy X-ray scattering measurements: 1, quartz tube; 2, thermocouple; 3, heater; 4, salt sample. Reprinted with permission from ref 61. Copyright 2020 American Chemical Society.

($S(q)$) and the pair distribution function (PDF) obtained via Fourier transformation of $S(q)$ are not quantities that are directly measured but instead are derived from experimental measurements of scattering intensity. Uncertainties or errors in $S(q)$ are often due to inaccuracies in intensity counting and approximations applied in data treatment. Specifically for molten salts, the rapid decay of the scattering intensity with increasing q, the low signal-to-background ratios (the total scattering signal for molten salt can be swamped by the scattering contributions of furnaces and containers) and difficulties in obtaining the structure factor to sufficiently high q-values can lead to problems in the determination of absolute normalizations and the subsequent derivation of high-resolution PDFs.

It is unfortunately not uncommon to see discrepancies in peak intensities between the X-ray/neutron $S(q)$ and PDF results reported by different research groups for a given molten salt system. These experimental inconsistences may cause uncertainty in the selection of the most reliable first-principles or classical force field methodology to interpret scattering and spectroscopic results from an atomistic perspective. To provide the most accurate experimental $S(q)$ values or PDFs, a wide range of experimental data for the same system and conditions would be desirable, including from different synchrotron/neutron sources, but such checks are scarce. In addition, direct $S(q)$/PDF comparisons with pioneering work in the literature are often also hindered by specific data treatments and processing protocols, e.g., different $S(q)$ normalization, the definition of the composition unit, and the use of modification functions. A particular sticking point is that pioneering work on molten salts was done using conventional X-ray and low flux neutron sources, leading to $S(q)$ functions with quite limited q-range and significant statistical errors. To highlight this point, Figure 4 compares our recent high-energy X-ray (74.4 keV)

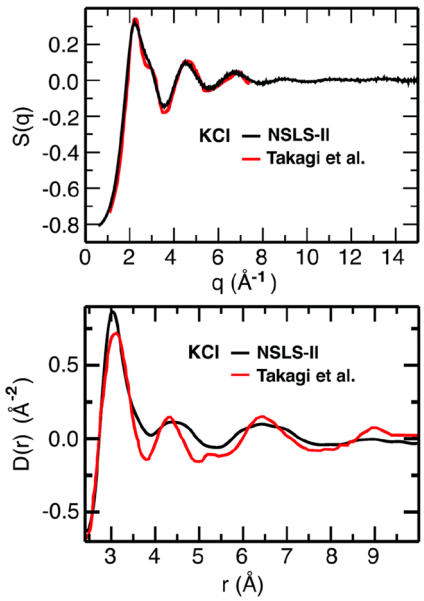

Figure 4. (Top) structure function, $S(q)$, recently obtained by our group at NSLS-II contrasted with that of Takagi et al.[28] (Bottom) Real space $D(r)$ functions derived from these. Reproduced from ref 95 with permission from the PCCP Owner Societies.

scattering results[95] for molten KCl obtained at the National Synchrotron Light Source II (NSLS-II) with those reported by Takagi et al.[28] using Cu Kα (8.0 keV) radiation. One may see noticeable discrepancies in the real-space PDF, $D(r)$, especially with respect to the positions and intensities of peaks associated with short-range order. These differences are crucially important when trying to understand coordination numbers and solvation environments for the ions. The observed inconsistencies are primarily due to termination errors at large q in Takagi's $S(q)$ data reported only up to q = 7.38 Å^{-1}—the highest momentum transfer attainable by the Cu Kα source in the range of the considered scattering angles.[28] Although the q-range for this earlier study is limited, the agreement with modern synchrotron measurements in the first three peaks of $S(q)$ is quite good, and this is particularly encouraging, since the structure functions were obtained from different instruments using different modes (reflection vs transmission), and as a consequence, they were derived through treatments in which various corrections had to be performed in different ways. The fact that, at least on a restricted q-range, pioneering results and data collected on more advanced synchrotron beamlines overlap provides confidence in the possibility to collect highly reproducible experimental data for molten salts which will serve as excellent benchmarks for theoretical models.

Computational Caveats and Considerations. Besides the obviously different temperature regimes on which

https://doi.org/10.1021/acs.jpcb.1c01065
J. Phys. Chem. B 2021, 125, 6359−6372

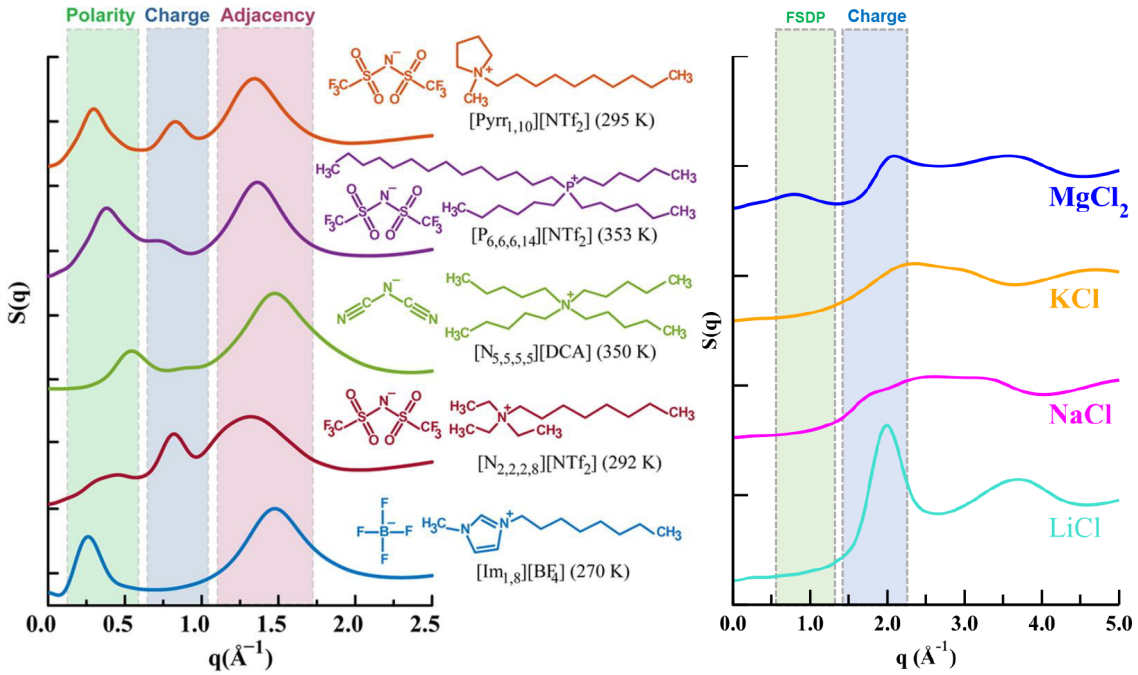

Figure 5. (Left) for different ILs, $S(q)$ highlighting regimes associated with polar−apolar alternation (this is the prepeak or first sharp diffraction peak), with charge alternation, and with vicinal adjacency correlations. (Right) for different molten salts, $S(q)$ highlighting the charge alternation region and when present the prepeak. Notice that charge alternation and prepeak regions occur at significantly higher q values for molten salts. Left panel reprinted with permission from ref 119. Copyright 2015 American Chemical Society.

measurements on IL and molten salt systems are carried out, from a computational perspective, a few other notable issues should be highlighted. In general, the lowest room-temperature IL viscosities are on the order of 10−20 times that of liquid water at atmospheric conditions, whereas other ILs have much higher viscosities that can be hundreds of cP or more.[108−110] Instead, high-temperature molten salts have low viscosities often on the order of 1 cP or sometimes less.[111,112] What this means is that from a computational perspective, guaranteed convergence of properties requires careful consideration in the case of ILs (simply put, simulations may require tens or hundreds of nanoseconds to converge depending on the property and temperature).[113,114] The issue of the high viscosity of ILs is compounded by the fact that force fields, particularly nonpolarizable force fields or those in which charges have not been scaled to account for some level of polarization or charge transfer, have actual model viscosities that are sometimes orders of magnitude larger than the experimental ones.[108,115] In other words, whereas an IL may be viscous but not in the glass regime, its fixed-charge force field model version may well be.

Yet, from a practical perspective particularly when interested in the structure function, models for ILs are much more forgiving than those for molten salts. What we mean by this is that whereas it is easy to get transport properties wrong (sometimes very wrong) for ILs, it is hard for a reasonable force field to not show the three typical characteristics of an IL: which are polar−apolar alternation [the so-called prepeak or first sharp diffraction peak (FSDP)], charge alternation, and adjacency correlations.[116−126] Each of these features appears in a specific q-range, as shown in Figure 5 (left).[119,127−134] Instead, structural properties of molten salts including coordination numbers and intermediate range order appear to be quite sensitive to the model and, as opposed to the case for ILs, it is very easy to get these wrong. Because of this, it is often the case that the Coulomb and dispersion-repulsion energy functions used for molten salts are more complex than those commonly used for ILs.[135] This is true even for the more complex force fields for ILs based on the polarizable Drude model.[115,136−142] The issue is most problematic when coupling small multivalent cations such as Mg^{2+} with highly polarizable anions such as Cl^-.[84,143] Because of the very short distance between these ions in the condensed phase, the physical validity of the commonly used point-induced dipole approximation within the polarizable ion model (PIM) requires careful consideration; this is less of an issue for ILs where interionic distances are larger and formal charges smeared over multiple atoms. To avoid unphysical overpolarization in the case of molten salts and to get structural and dynamical properties right, the key ingredient is the collection of pairwise damping functions used to correct the charge-induced dipole interactions.[53−58,61,84] This often results in force field parameters that are only good to simulate a specific system but are not easily transferable. In other words, for molten salts with multivalent cations and polarizable anions, do not expect to find parameters for a given ion in the literature and assume that those can be trivially combined with other parameters even when the force field has the same functional form. Because of their low viscosity, the number of nanoseconds in a molecular dynamics simulation run needed to converge molten salts properties are in general lower than for ILs but actual wall times tend to be comparable or even longer due to the complexity of force fields.[84]

Why Are Features in $S(q)$, Particularly Those Associated with the FSDP, Much More Sensitive to the Force Field in the Case of Inorganic Molten Salts?

Let us consider a prototypical ionic liquid such as $[C_n\text{mim}][PF_6]$, below $n = 4$ the first sharp diffraction peak is not prominent or observed and for $n = 6$, 8, 16 the prepeak is at q

https://doi.org/10.1021/acs.jpcb.1c01065
J. Phys. Chem. B 2021, 125, 6359−6372

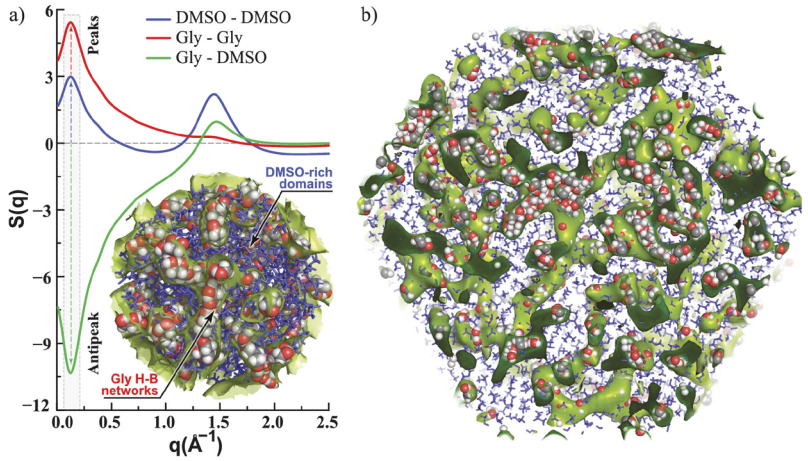

Figure 6. (Left) partial subcomponents of $S(q)$ for a mixture of the conventional solvents dimethyl sulfoxide and glycerol. The figure highlights the two peaks and one antipeak associated with the pattern of alternation associated with the distance between glycerol chains spaced by dimethyl sulfoxide domains; (right) a larger view of the system highlighting these alternations in real space.[147] Reprinted with permission from ref 147. Copyright 2015 American Chemical Society.

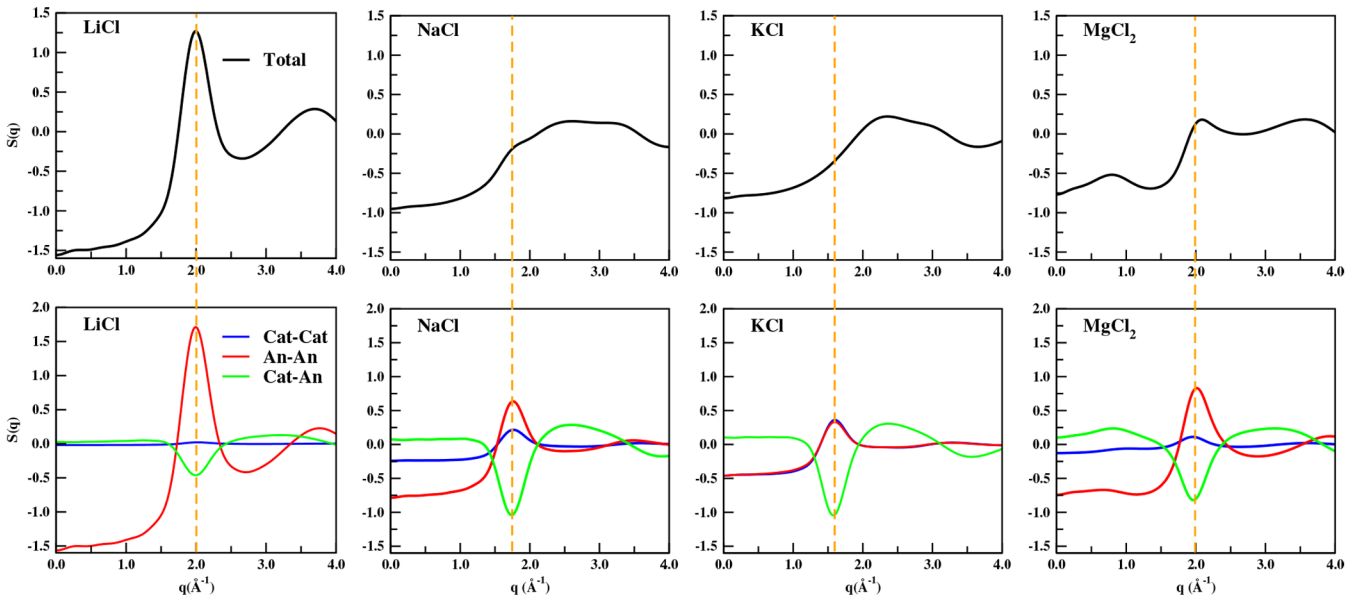

Figure 7. For LiCl, NaCl, KCl, and $MgCl_2$, (top) total $S(q)$ and (bottom) partial subcomponents of $S(q)$. A vertical dashed line highlights how the sum of two peaks and one antipeak in some cases results in a peak in the overal $S(q)$ but in others there is a shoulder or even no noticeable feature due to cancellations. Data for LiCl is at 1148 K, KCl at 1173 K, and $MgCl_2$ at 1073 K.[61,95]

= 0.350, 0.297, and 0.183 Å^{-1} respectively.[144] How bad would a force field need to be in order to produce a prepeak that is off by about 0.1 Å^{-1} in the case of $[C_{16}mim][PF_6]$? A trivial estimation for the periodicity of the prepeak is $2\pi/0.183 \approx 34.33$ Å; a shift to the left by 0.1 Å^{-1} would result in $2\pi/0.083 \approx 75.70$ Å. This is about 40 Å off in real space! Instead, if we consider $MgCl_2$ where the prepeak appears at 0.85 Å^{-1},[58] the same shift in q would result in a real space distance difference of about 1 Å; $2\pi/0.85 \approx 7.39$ Å whereas $2\pi/0.75 \approx 8.38$ Å. In other words, most reasonable force fields for ILs will get the prepeak position correctly, but instead, small changes in a force field can have major consequences on the shape and position of the features in $S(q)$ for a typical molten salt.

The Defining Feature for Molten Salts Is the Two Peaks and One Antipeak Associated With Charge Alternation. Many times but not always, a peak in the overall $S(q)$ corresponding to charge alternation is prominent and called "the main peak" in the literature.[145,146] However, in other cases this peak is completely absent and the main peak has a different structural origin. This is true both for molten salts and for ILs. We see this clearly from Figure 5 (left) where $[Im_{1,8}][BF_4]$ shows no peak in the charge alternation region around 0.8 Å^{-1} but $[N_{2,2,2,8}][NTf_2]$ shows a prominent peak; we also see this from Figure 5 (right) where for KCl there is no sign of a peak around 1.8 Å^{-1} but LiCl shows a prominent peak just below 2 Å^{-1}. The key point is that all molten salts and ILs are defined by charge alternation, but *whether the charge alternation peak is prominent or completely absent is simply a matter of contrast in the technique.*[116]

We begin to understand this when we notice that for any liquid, alternations at any particular length scale are associated with two peaks and one antipeak in the partial subcomponents

https://doi.org/10.1021/acs.jpcb.1c01065
J. Phys. Chem. B 2021, 125, 6359−6372

of $S(q)$ in the same q region.[116,119] For example, a mixture of glycerol and DMSO can become nanoheterogeneous with nanoscopic chains of glycerol spaced by DMSO domains, as can be seen in Figure 6. The typical distance between two glycerol chains is about the same as the typical distance between DMSO domains intercalated by a glycerol chain. This results in a peak at low q values for the DMSO−DMSO subcomponent of $S(q)$ and another peak in the same region for the glycerol−glycerol subcomponent. Because the two patterns of alternation in the case of glycerol and DMSO are shifted by half a period (DMSO domains are intercalated by glycerol chains and glycerol chains are separated by DMSO domains) the DMSO−glycerol subcomponent of $S(q)$ appears as an antipeak or a negative going peak at the same q region. The concept is the same for any other type of alternation and certainly applies to the charge alternation behavior of molten salts and ILs albeit at a larger q value.[116]

Whether these peaks and antipeaks are prominent in the subcomponents of $S(q)$ depends on the corresponding values of the X-ray atomic form factors or neutron scattering lengths. This is clearly depicted in Figure 7 where for KCl the formal number of electrons for K^+ and Cl^- are the same and the ionic sizes are very similar, hence the q-dependent form factors are also quite similar. The two peaks (K−K and Cl−Cl) superpose, and the K−Cl antipeak completely cancels them.[95] This results in large partial subcomponents of the structure factor completely canceling out to yield an X-ray $S(q)$ that is featureless in the charge alternation regime! The opposite is true for LiCl where there is significant difference in the size and number of electrons of the species creating contrast between the anion and the cation that translates into an easily observable charge alternation peak in the overall $S(q)$. The cases of NaCl and $MgCl_2$ are intermediate between these two where the contrast is reasonable in the case of $MgCl_2$ and a prominent peak is observed but only a shoulder appears in the overall $S(q)$ for NaCl. Because neutron scattering and X-ray scattering depend on the details of the nuclear structure of the species in one case and the electronic structure of the species in the other, a charge alternation peak that is completely absent in the X-ray $S(q)$ can be prominent in the neutron $S(q)$. In conclusion, all molten salts are characterized by charge alternation in the subcomponents of $S(q)$, but only in some cases these do not cancel and give rise to a prominent main charge alternation peak in the overall X-ray or neutron $S(q)$. It is not safe to assume that the main peak is always associated with charge alternation, but it is safe to assume that if a charge alternation peak is not present in $S(q)$, this is simply due to a technique limitation and not due to lack of charge alternation in the condensed phase.

How are ionic liquids different or similar to molten salts when thinking about charge alternation? When we think of molten salts, we envision single-atom cations and anions that alternate in a 3D pattern linked to their relative sizes, polarizabilities, formal charges, etc. Instead, in the case of prototypical ILs, it is often the cation that has a "polar head" and an "apolar tail", and it is the cation polar head and not the full cation that alternates with the anions, which are often but not always symmetrical and without an apolar component[117,121,122,125,126] (some anions are asymmetric and can have extensive fluorinated or other type of tails, but this is not the subject of our discussion). It is then the cation head−cation head and the anion−anion subcomponents of $S(q)$ that manifest as peaks in the charge alternation reciprocal space region and the cation head−anion subcomponents that show as an antipeak. Notice that this charge alternation region in reciprocal space is at significantly different q values for ILs and molten salts (≈0.8 $Å^{-1}$ in Figure 5 (left) and ≈1.8 $Å^{-1}$ in Figure 5 (right), respectively). We emphasize again that it is easier for force fields of ionic liquids to capture this feature correctly as it appears at significantly smaller q values (larger distances). All other considerations are the same as described in the paragraph above. All ionic liquids and molten salts display charge alternation, but only in some cases this shows in the overall neutron or X-ray scattering $S(q)$ due to contrast.[121]

Intermediate Range Order for Molten Salts. In the early 2010s, there was significant controversy regarding the origin of the prepeak in ILs.[117,144,148−150] In hindsight, and for prototypical ILs, this problem is very simple and has been fully resolved.[116,119,129,144,151−186] For ILs, where cations have a charged head and a significantly large apolar tail, the prepeak is due to the typical distance between charge networks alternated by apolar regions, or apolar domains alternated by the charge network.[116−126] Since this is a pattern of alternation, same type species (polar−polar and apolar−apolar) show peaks in partial subcomponents of $S(q)$ at the prepeak region, whereas opposite type species (polar−apolar) show an antipeak; notice that positive and negative species are considered "same type species" in this q regime because they are both polar.[123,124] This is clearly depicted in Figure 8, where polar cationic and anionic heads form networks that are separated by other networks via tails that act as spacers.

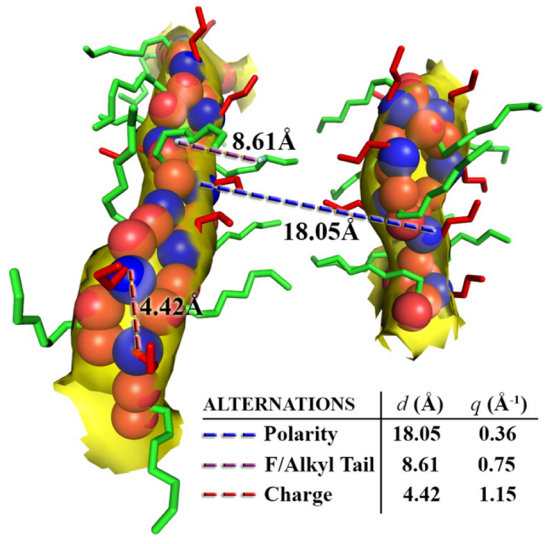

Figure 8. For an ionic liquid, two charge networks spaced by tails.[122] Reprinted with permission from ref 122. Copyright 2014 American Chemical Society.

Pinpointing the origin of intermediate range order in the case of molten salts is significantly more difficult. Molten salts do not have apolar regions, and the prepeak does not necessarily stem from a simple pattern of alternation with two peaks and an antipeak in the partial subcomponents of $S(q)$ as in the case for ILs. The reader can immediately see the absence of this pattern from the subcomponents of $S(q)$ for $MgCl_2$ in Figure 7 at about 0.85 $Å^{-1}$.

So what gives rise to a prepeak in molten salts? This has been studied extensively and a particularly good discussion can be found in a review article by Wilson.[187] Our group has

https://doi.org/10.1021/acs.jpcb.1c01065
J. Phys. Chem. B 2021, 125, 6359−6372

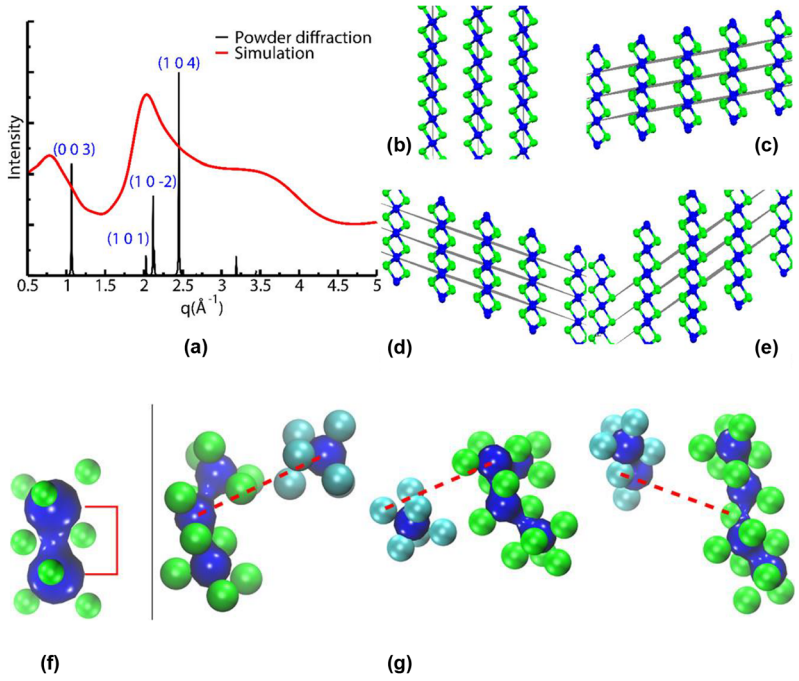

Figure 9. (a) Powder diffraction peaks and liquid phase intensity for $MgCl_2$. (b) (003), (c) $(10\bar{2})$, (d) (101), and (e) (104) Bragg planes in the $MgCl_2$ crystal. Planes (003) exemplify across network prepeak behavior, $(10\bar{2})$ and (101) planes charge alternation behavior, and (104) planes are one of the many possible examples of adjacency correlations. (f) Depicted as a surface two Mg^{2+} ions sharing at their waist Cl^- counterions (charge alternation behavior). (g) Examples of across network interactions (prepeak behavior). Top figure reprinted with permission from ref 58 and bottom figure reprinted with permission from ref 61. Copyrights 2019 and 2020 American Chemical Society.

studied the case of $MgCl_2$ and its mixtures with KCl and what we found is that $MgCl_2$ is a networked liquid with chains of Cl^--decorated Mg^{2+} ions.[58,61,84] These in-network Mg^{2+} ions share Cl^- counterions, but there are nearby Mg^{2+} ions that are either part of a different network or simply form a cluster and do not share Cl^- counterions with the first network. The distance between Mg^{2+} ions sharing counterions is different from that of those not sharing counterions. The first distance, which is shorter, has to do with the charge alternation feature in $S(q)$, whereas the second has to do with the prepeak.[61] In other words, just like in the case of ILs, the prepeak has to do with the distance between charge networks. In the case of ILs these charge networks are spaced by tail domains, but in the case of $MgCl_2$ there is no spacer. Whereas these two characteristic distances in the case of $MgCl_2$ are different, the difference is not very large when contrasted with the difference between typical charge alternation vs polarity alternation distances for ILs. Being able to resolve these differences computationally in the case of molten salts depends on the intricacies of the polarizable force field and damping functions. In general, our experience is that nonpolarizable force fields or core−shell type models are unable to do so but our recently developed SEM-Drude model which uses charge-dipole damping functions akin to those in the more expensive PIM can. Perhaps, one could come up with a clever way to partition and label ion collections to see the prepeak of molten salts as an alternation pattern. However, this would be computationally impractical because such labels would necessarily change from simulation frame to simulation frame, and as opposed to the case for ILs, they would be ion location-dependent instead of ion type-dependent.

Perhaps the best way to begin understanding the structure of the $MgCl_2$ melt and in particular the origin of the prepeak is by looking at its crystal structure in Figure 9. Here, we do not mean to imply that the melt is a disordered version of the crystal. Instead, what we claim is that features in the melt are reminiscent of those in the crystal, which can also be described as having Cl^--decorated Mg^{2+} networks in which the distance between adjacent cations that are in-network is different from that of adjacent cations that are across networks. The (003) planes shown in Figure 9b are the lowest observed q planes, and atoms associated with these planes resemble those associated with the prepeak in the liquid phase (see Figure 9g). These planes go through the Cl-decorated Mg^{2+} charge networks and the distance between planes is the distance between the networks. Notice that there is no sharing of Cl^- counterions across networks, only along networks. If we compare the FSDP in the crystal with that of the red line associated with the melt in Figure 9a, it is obvious that the prepeak appears at lower q values (longer distance) in the disordered phase; this is to be expected because of the lower density of the liquid phase. In the liquid phase, networks are shorter and randomly distributed and the coordination number of Mg^{2+} is lower than in the crystal, yet for practical purposes the prepeak has a similar origin in both phases. Notice also that Figure 9c,d are instances of what in the previous section we defined as charge alternation behavior (i.e., the typical distance between in-network cations that share counterions like in Figure 9f of the melt). Instead, Figure 9e represents one of the many possible version of what we have called in the past[58,117,124] adjacency correlations since the distance between planes is associated with the distance between adjacent cations and anions.

Effects of Temperature and Dilution on the Prepeak. It is intuitive to expect features in $S(q)$ to become less intense as the temperature increases; this, after all, is typical Debye−

https://doi.org/10.1021/acs.jpcb.1c01065
J. Phys. Chem. B 2021, 125, 6359−6372

Waller behavior. Yet, both for ILs and molten salts the prepeak is special in that one commonly finds non-Debye–Waller behavior; see, for example, ref 188 in the case of ILs and ref 61 in the case of molten salts. In the case of $MgCl_2$, two patterns govern the topology of the liquid state. The first pattern is the charge alternation along networks and the second pattern is the typical distance between or across these networks. As temperature increases, the likelyhood of long chains of Mg^{2+} that share Cl^- counterions diminishes; this results in the expected Debye–Waller behavior for $S(q)$ in the charge alternation region around 2 $Å^{-1}$. Concomitant with a decrease in the prevalence of corner- or edge-sharing[189] Cl^--decorated Mg^{2+} networks, the likelihood of finding nearby cations that do not share counterions, associated with the prepeak, becomes larger. At least in the case of $MgCl_2$, this statistical effect of fewer in-network interactions and more across-network interactions appears to be the reason for the Debye–Waller behavior of the charge alternation peak and the non-Debye–Waller behavior of the prepeak.

Figure 10 shows the probability of Cl^--decorated Mg^{2+} aggregate sizes as a function of temperature; the left panel highlights the smaller networks side of the distribution and the right panel the larger networks. The effect of temperature is as expected from the Debye–Waller behavior of the charge alternation peak in $S(q)$; larger networks disappear at high T. The reader is asked to compare these graphs with those in Figure 11 where the size of Mg^{2+} aggregates is studied as a function of dilution with KCl. We see from Figure 11 that the monovalent salt acts as a powerful Mg^{2+} network disruptor with significant implications on transport properties such as viscosity.

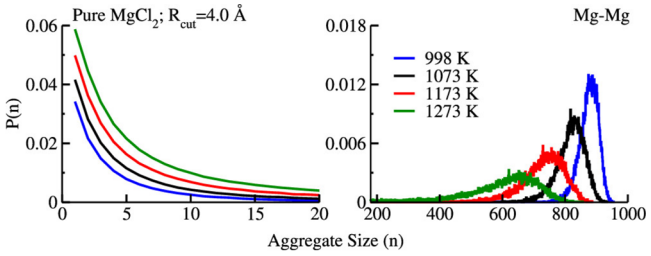

Figure 10. Probability of Cl^--decorated Mg^{2+} aggregates as a function of temperature. Reprinted with permission from ref 84. Copyright 2020 American Chemical Society.

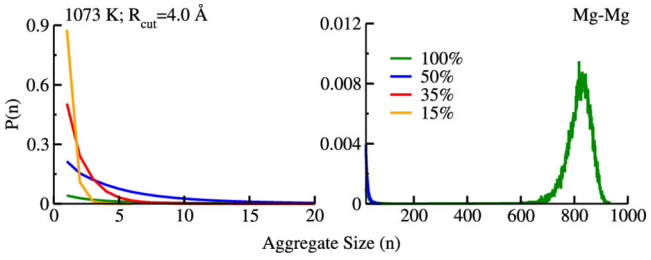

Figure 11. For 1073 K, probability of Cl^--decorated Mg^{2+} aggregates as a function of dilution. At 100 mol % $MgCl_2$ there is a significant probability of large aggregate sizes, but the probability decreases rapidly upon dilution. Reprinted with permission from ref 84. Copyright 2020 American Chemical Society.

CONCLUSIONS

Ionic liquids and high-temperature inorganic molten salts share many characteristics but are also different in important ways. Molten salts exist in a regime of low viscosities whereas ILs are often much more viscous. From a structural perspective, both are characterized by charge alternation, a feature that always manifests in the partial subcomponents of $S(q)$ as two peaks and one antipeak. Whether the sum of these components results in a peak in the overal $S(q)$ depends mostly on contrast from the specific scattering technique. Some ionic liquids and molten salts also display a first sharp diffraction peak. In the case of the most common ILs, this feature is simply due to polarity alternation; this is the pattern of apolar domains separated by charge networks or that of charge networks intercalated by apolar domains. For molten salts, the origin of the prepeak is more complex as it does not trivially arise from an alternation of same-type and opposite-type species. Yet, it would appear that at least in some cases, the separation between charge networks (albeit without a molecular spacer) is also the origin of the prepeak for molten salt systems. *In this case the two typical length scales, associated with the in-network charge alternation peak and the across network prepeak, simply differ because of the way multivalent cations are solvated by counterions*. The charge alternation peak is associated with cations that, because they belong to the same network, necessarily share counterions; the prepeak instead is associated with cations that are also close in distance but are each solvated by a distinct set of anions. These two characteristic distances are difficult if not impossible for nonpolarizable force fields to capture without the use of extraneous terms in the potential. Even polarizable force fields require damping functions in the charge-induced dipole terms to accurately reproduce the two distinct length scales. This brings us to the topic of force field accuracy and transferability, which is much more of a problem for high-temperature molten salts than for ILs. For ILs, features in $S(q)$ occur at significantly lower q values than the same features in the case of molten salts. This means that small inconsistencies across force fields will result in minor changes in $S(q)$ for ILs but can wreak havoc in the subtle balance of shorter distances that cause the periodicities associated with peaks in $S(q)$ for molten salts. For molten salts with small multivalent ions and polarizable counterions, the classical point-induced dipole approximation fails and complex corrections are required to reproduce quantum mechanical results and capture features like the prepeak in $S(q)$. In the case of ILs, polarization is also important, particularly to properly capture transport properties, but structural properties are less sensitive to the details of the force field. This is in part because the distance between ions is larger and also because formal charges are smeared across atoms in the case of ILs. These are in fact some of the features that make salts composed of these larger and softer ions liquid at room temperature.

Whereas measurements on ILs can be difficult due to their hygroscopicity, the same measurements for high-temperature molten salts have the extra complexities associated with impurity reactivity, the need for special setups and the background signal of furnaces among other issues. Furthermore, a significant fraction of these complex measurements have been done in the past using pioneering instruments that among other issues do not go to the large q values that current facilities can achieve. This becomes an issue because often $S(q)$

https://doi.org/10.1021/acs.jpcb.1c01065
J. Phys. Chem. B 2021, 125, 6359–6372

is not flat at the cuttoff point and inversion of the data to obtain real space PDFs becomes problematic. The consequence of this is real space data deeply entrenched in the literature, such as coordination numbers for the ions and solvation geometries, that may need to be revisited. This offers tremendous opportunities to impact atomic and quasi-chemical models needed to predict properties, some of them very difficult to measure for molten salt systems.

AUTHOR INFORMATION

Corresponding Authors

Alexander S. Ivanov − *Chemical Sciences Division, Oak Ridge National Laboratory, Oak Ridge, Tennessee 37830, United States;* orcid.org/0000-0002-8193-6673; Email: ivanova@ornl.gov

Claudio J. Margulis − *Department of Chemistry, The University of Iowa, Iowa City, Iowa 52242, United States;* orcid.org/0000-0003-1671-9784; Email: claudio-margulis@uiowa.edu

Author

Shobha Sharma − *Department of Chemistry, The University of Iowa, Iowa City, Iowa 52242, United States;* orcid.org/0000-0002-5459-7215

Complete contact information is available at: https://pubs.acs.org/10.1021/acs.jpcb.1c01065

Notes

The authors declare no competing financial interest.

Biographies

Shobha Sharma earned her B.Sc. (Life Sciences) from Miranda House, University of Delhi, Delhi. After completing her M.Sc. (Chemistry) from GJUS&T, Hisar, she received a Ph.D. from the Indian Institute of Technology Delhi under the supervision of Dr. Hemant K. Kashyap. Currently, she is a postdoctoral scholar at the University of Iowa working with Prof. Claudio J. Margulis. Her research interests are mainly focused on investigating the structure and dynamics of high temperature molten salts and ionic liquids using molecular dynamics simulations.

Alexander S. Ivanov is a Research Scientist in the Chemical Sciences Division at Oak Ridge National Laboratory. He received his Ph.D. from Utah State University in 2015. Dr. Ivanov's research lies broadly in the development and application of neutron/X-ray scattering techniques and theoretical methods to investigate processes and functional materials for energy-relevant technologies, including chemical separations, molecular recognition, catalysis, and sustainability. His recent projects include experimental investigations of the structural and dynamic properties of molten salts using total scattering techniques, and he is also currently involved in a collaboration with industrial partners focusing on the development of molten salt nanofluids for advanced nuclear reactors.

Claudio Javier Margulis received a Licenciado en Ciencias Químicas degree from The University of Buenos Aires in 1996 and a Ph.D. from Boston University in 2001. He did postdoctoral work at Columbia University between 2001 and 2003 until he joined the Department of Chemistry at the University of Iowa where he is currently a Professor. His research focuses on computational and theoretical studies of molten salts and ionic liquids.

ACKNOWLEDGMENTS

This work was supported as part of the Molten Salts in Extreme Environments (MSEE) Energy Frontier Research Center, funded by the U.S. Department of Energy Office of Science. MSEE work at the University of Iowa was supported via subcontracts from Brookhaven National Laboratory, which is operated under DOE Contract No. DE-SC0012704. Oak Ridge National Laboratory is operated under DOE Contract No. DE-AC05-00OR22725. Being a perspectives article, this work discusses data and includes figures published previously

by us and others. Funding sources for those works were acknowledged in the original publications.

REFERENCES

(1) Zachariasen, W. H. The vitreous state. *J. Chem. Phys.* **1935**, *3*, 162.
(2) Herzfeld, K. F. The liquid state. *J. Appl. Phys.* **1937**, *8*, 319.
(3) Warren, B. E. X-ray diffraction study of the structure of glass 1. *Chem. Rev.* **1940**, *26*, 237−255.
(4) Warren, B. E. Summary of work on atomic arrangement in glass. *J. Am. Ceram. Soc.* **1941**, *24*, 256−261.
(5) Taylor, N. W. Anomalous flow in glasses. *J. Phys. Chem.* **1943**, *47*, 235−253.
(6) Mulcahy, M. F. R.; Heymann, E. On the nature of molten salts and their mixtures1. *J. Phys. Chem.* **1943**, *47*, 485−496.
(7) Stevels, J. M. The physical properties of glass II: The density of silicate glasses. *Recueil des Travaux Chimiques des Pays-Bas* **1943**, *62*, 17−27.
(8) Fajans, Kasimir; Kreidl, N. J. Stability of lead glasses and polarization of ions. *J. Am. Ceram. Soc.* **1948**, *31*, 105−114.
(9) Briant, R. C.; Weinberg, A. M. Molten fluorides as power reactor fuels. *Nucl. Sci. Eng.* **1957**, *2*, 797−803.
(10) Levy, H. A.; Agron, P. A.; Bredig, M. A.; Danford, M. D. X-ray and neutron diffraction studies of molten alkali halides. *Ann. N. Y. Acad. Sci.* **1960**, *79*, 762−780.
(11) Fumi, F.; Tosi, M. Ionic sizes and born repulsive parameters in the NaCl-type alkali halides-I: The Huggins-Mayer and Pauling forms. *J. Phys. Chem. Solids* **1964**, *25*, 31−43.
(12) Schröder, U. A new model for lattice dynamics ("breathing shell model"). *Solid State Commun.* **1966**, *4*, 347−349.
(13) Basu, A. N.; Sengupta, S. A deformable shell model for the alkali halides. *Phys. Status Solidi B* **1968**, *29*, 367−375.
(14) Haubenreich, P. N.; Engel. Experience with the molten-salt reactor experiment. *Nucl. Appl. Technol.* **1970**, *8*, 118−136.
(15) Woodcock, L. V.; Singer, K. Thermodynamic and structural properties of liquid ionic salts obtained by Monte Carlo computation. Part 1.-Potassium chloride. *Trans. Faraday Soc.* **1971**, *67*, 12−30.
(16) Maroni, V. A. Vibrational frequencies and force constants for tetrahedral MgX (X = Cl, Br, and I) in MgX_2−KX melts. *J. Chem. Phys.* **1971**, *55*, 4789−4792.
(17) Maroni, V. A.; Hathaway, E. J.; Cairns, E. J. Structural studies of magnesium halide-potassium halide melts by Raman spectroscopy. *J. Phys. Chem.* **1971**, *75*, 155−159.
(18) Capwell, R. Raman spectra of crystalline and molten $MgCl_2$. *Chem. Phys. Lett.* **1972**, *12*, 443−446.
(19) Adams, D. J.; McDonald, I. R. Rigid-ion models of the interionic potential in the alkali halides. *J. Phys. C: Solid State Phys.* **1974**, *7*, 2761−2775.
(20) Basu, A. N.; Roy, D.; Sengupta, S. Polarisable models for ionic crystals and the effective many-body interaction. *Phys. Status Solidi A* **1974**, *23*, 11−32.
(21) Lewis, J. W. E.; Singer, K.; Woodcock, L. V. Thermodynamic and structural properties of liquid ionic salts obtained by Monte Carlo computation. Part 2.-Eight alkali metal halides. *J. Chem. Soc., Faraday Trans. 2* **1975**, *71*, 301−312.
(22) Brooker, M. H. A Raman spectroscopic study of the structural aspects of K_2MgCl_4 and Cs_2MgCl_4 as solid single crystals and molten salts. *J. Chem. Phys.* **1975**, *63*, 3054.
(23) Huang, C.-H.; Brooker, M. Raman spectrum of molten $MgCl_2$. *Chem. Phys. Lett.* **1976**, *43*, 180−182.
(24) Sangster, M.; Dixon, M. Interionic potentials in alkali halides and their use in simulations of the molten salts. *Adv. Phys.* **1976**, *25*, 247−342.
(25) Jacucci, G.; McDonald, I. R.; Rahman, A. Effects of polarization on equilibrium and dynamic properties of ionic systems. *Phys. Rev. A: At., Mol., Opt. Phys.* **1976**, *13*, 1581−1592.
(26) Catlow, C. R. A.; Diller, K. M.; Norgett, M. J. Interionic potentials for alkali halides. *J. Phys. C: Solid State Phys.* **1977**, *10*, 1395−1412.
(27) Sangster, M. J.; Atwood, R. M.; Schroder, U. Interionic potentials for alkali halides. I. Crystal independent shell parameters and fitted Born-Mayer potentials. *J. Phys. C: Solid State Phys.* **1978**, *11*, 1523−1540.
(28) Takagi, R.; Ohno, H.; Furukawa, K. Structure of molten KCl. *J. Chem. Soc., Faraday Trans. 1* **1979**, *75*, 1477−1486.
(29) Brooker, M. H.; Huang, C.-H. Raman spectroscopic studies of structural properties of solid and molten states of the magnesium chloride − alkali metal chloride system. *Can. J. Chem.* **1980**, *58*, 168−179.
(30) Biggin, S.; Enderby, J. E. The structure of molten zinc chloride. *J. Phys. C: Solid State Phys.* **1981**, *14*, 3129−3136.
(31) Busse, L. E.; Nagel, S. R. Temperature dependence of the structure factor of As_2Se_3 glass up to the glass transition. *Phys. Rev. Lett.* **1981**, *47*, 1848−1851.
(32) Dixon, M.; Gillan, M. J. Structure of molten alkali chlorides. *Philos. Mag. B* **1981**, *43*, 1099−1112.
(33) Biggin, S.; Enderby, J. E. Comments on the structure of molten salts. *J. Phys. C: Solid State Phys.* **1982**, *15*, L305−L309.
(34) Biggin, S.; Gay, M.; Enderby, J. E. The structures of molten magnesium and manganese (II) chlorides. *J. Phys. C: Solid State Phys.* **1984**, *17*, 977−985.
(35) Busse, L. E. Temperature dependence of the structures of As_2Se_3 and As_xS_{1-x} glasses near the glass transition. *Phys. Rev. B: Condens. Matter Mater. Phys.* **1984**, *29*, 3639−3651.
(36) Newport, R. J.; Howe, R. A.; Wood, N. D. The structure of molten nickel chloride. *J. Phys. C: Solid State Phys.* **1985**, *18*, 5249−5257.
(37) de Wette, F. W.; Kress, W.; Schröder, U. Relaxation of the rocksalt (001) surface: Alkali halides, MgO, and PbS. *Phys. Rev. B: Condens. Matter Mater. Phys.* **1985**, *32*, 4143−4157.
(38) McGreevy, R. L.; Mitchell, E. W. J. Collective modes in molten alkaline earth chlorides: III. Inelastic neutron scattering from molten $MgCl_2$ and $CaCl_2$. *J. Phys. C: Solid State Phys.* **1985**, *18*, 1163−1178.
(39) Revere, M.; Tosi, M. P. Structure and dynamics of molten salts. *Rep. Prog. Phys.* **1986**, *49*, 1001−1081.
(40) Mamantov, G.; Marassi, R. *Molten salt chemistry: An introduction and selected applications*; Springer, 1987.
(41) Kumta, P.; Deymier, P.; Risbud, S. Improved rigid ion model of molten zinc chloride. *Phys. B* **1988**, *153*, 85−92.
(42) Board, J. A.; Elliott, R. J. Shell model molecular dynamics calculations of the Raman spectra of molten NaI. *J. Phys.: Condens. Matter* **1989**, *1*, 2427−2440.
(43) McGreevy, R. L.; Pusztai, L. The structure of molten salts. *Proc. R. Soc. London A* **1990**, *430*, 241−261.
(44) O'Sullivan, K. F.; Madden, P. A. Light scattering by alkali halides melts: a comparison of shell-model and rigid-ion computer simulation results. *J. Phys.: Condens. Matter* **1991**, *3*, 8751−8756.
(45) Wilson, M.; Madden, P. A. Short- and intermediate-range order in MCl_2 melts: the importance of anionic polarization. *J. Phys.: Condens. Matter* **1993**, *5*, 6833−6844.
(46) Mitchell, P. J.; Fincham, D. Shell model simulations by adiabatic dynamics. *J. Phys.: Condens. Matter* **1993**, *5*, 1031−1038.
(47) Lindan, P. J. D.; Gillan, M. J. Shell-model molecular dynamics simulation of superionic conduction in CaF_2. *J. Phys.: Condens. Matter* **1993**, *5*, 1019−1030.
(48) Fincham, D.; Mackrodt, W. C.; Mitchell, P. J. MgO at high temperatures and pressures: shell-model lattice dynamics and molecular dynamics. *J. Phys.: Condens. Matter* **1994**, *6*, 393−404.
(49) Wilson, M.; Madden, P. A. Anion polarization and the stability of layered structures in MX_2 systems. *J. Phys.: Condens. Matter* **1994**, *6*, 159−170.
(50) Wilson, M.; Madden, P. A. Prepeaks and first sharp diffraction peaks in computer simulations of strong and fragile ionic liquids. *Phys. Rev. Lett.* **1994**, *72*, 3033−3036.
(51) Wilson, M.; Madden, P. A.; Costa-Cabral, B. J. Quadrupole polarization in simulations of ionic systems: Application to AgCl. *J. Phys. Chem.* **1996**, *100*, 1227−1237.

https://doi.org/10.1021/acs.jpcb.1c01065
J. Phys. Chem. B 2021, 125, 6359−6372

(52) Wilson, M.; Madden, P. A. Voids, layers, and the first sharp diffraction peak in $ZnCl_2$. *Phys. Rev. Lett.* **1998**, *80*, 532−535.
(53) Wilson, M. Extended ionic models from *ab initio* calculations. *Philos. Trans. R. Soc., A* **2000**, *358*, 399−418.
(54) Ohtori, N.; Salanne, M.; Madden, P. A. Calculations of the thermal conductivities of ionic materials by simulation with polarizable interaction potentials. *J. Chem. Phys.* **2009**, *130*, 104507.
(55) Salanne, M.; Madden, P. A. Polarization effects in ionic solids and melts. *Mol. Phys.* **2011**, *109*, 2299−2315.
(56) Salanne, M.; Marrocchelli, D.; Merlet, C.; Ohtori, N.; Madden, P. A. Thermal conductivity of ionic systems from equilibrium molecular dynamics. *J. Phys.: Condens. Matter* **2011**, *23*, 102101.
(57) Ishii, Y.; Kasai, S.; Salanne, M.; Ohtori, N. Transport coefficients and the Stokes−Einstein relation in molten alkali halides with polarisable ion model. *Mol. Phys.* **2015**, *113*, 2442−2450.
(58) Wu, F.; Roy, S.; Ivanov, A. S.; Gill, S. K.; Topsakal, M.; Dooryhee, E.; Abeykoon, M.; Kwon, G.; Gallington, L. C.; Halstenberg, P.; et al. Elucidating ionic correlations beyond simple charge alternation in molten $MgCl_2$-KCl mixtures. *J. Phys. Chem. Lett.* **2019**, *10*, 7603−7610.
(59) Walz, M. M.; Van Der Spoel, D. Molten alkali halides-temperature dependence of structure, dynamics and thermodynamics. *Phys. Chem. Chem. Phys.* **2019**, *21*, 18516−18524.
(60) Kurley, J. M.; Halstenberg, P. W.; McAlister, A.; Raiman, S.; Dai, S.; Mayes, R. T. Enabling chloride salts for thermal energy storage: implications of salt purity. *RSC Adv.* **2019**, *9*, 25602−25608.
(61) Wu, F.; Sharma, S.; Roy, S.; Halstenberg, P.; Gallington, L. C.; Mahurin, S. M.; Dai, S.; Bryantsev, V. S.; Ivanov, A. S.; Margulis, C. J. Temperature dependence of short and intermediate range order in molten $MgCl_2$ and its mixture with KCl. *J. Phys. Chem. B* **2020**, *124*, 2892−2899.
(62) Gill, S. K.; Huang, J.; Mausz, J.; Gakhar, R.; Roy, S.; Vila, F.; Topsakal, M.; Phillips, W. C.; Layne, B.; Mahurin, S.; et al. Connections between the speciation and solubility of Ni(II) and Co(II) in molten $ZnCl_2$. *J. Phys. Chem. B* **2020**, *124*, 1253−1258.
(63) Ronne, A.; He, L.; Dolzhnikov, D.; Xie, Y.; Ge, M.; Halstenberg, P.; Wang, Y.; Manard, B. T.; Xiao, X.; Lee, W.-K.; et al. Revealing 3D morphological and chemical evolution mechanisms of metals in molten salt by multimodal microscopy. *ACS Appl. Mater. Interfaces* **2020**, *12*, 17321−17333.
(64) Antonelli, S.; Ronne, A.; Han, I.; Ge, M.; Layne, B.; Shahani, A. J.; Iwamatsu, K.; Wishart, J. F.; Hulbert, S. L.; Lee, W.-K.; et al. Versatile compact heater design for in situ nano-tomography by transmission X-ray microscopy. *J. Synchrotron Radiat.* **2020**, *27*, 746−752.
(65) Phillips, W. C.; Gakhar, R.; Horne, G. P.; Layne, B.; Iwamatsu, K.; Ramos-Ballesteros, A.; Shaltry, M. R.; LaVerne, J. A.; Pimblott, S. M.; Wishart, J. F. Design and performance of high-temperature furnace and cell holder for in situ spectroscopic, electrochemical, and radiolytic investigations of molten salts. *Rev. Sci. Instrum.* **2020**, *91*, 083105.
(66) Gill, S. K.; Sure, J.; Wang, Y.; Layne, B.; He, L.; Mahurin, S.; Wishart, J. F.; Sasaki, K. Investigating corrosion behavior of Ni and Ni-20Cr in molten $ZnCl_2$. *Corros. Sci.* **2021**, *179*, 109105.
(67) Dias, E. T.; Gill, S. K.; Liu, Y.; Halstenberg, P.; Dai, S.; Huang, J.; Mausz, J.; Gakhar, R.; Phillips, W. C.; Mahurin, S. Radiation-assisted formation of metal nanoparticles in molten salts. *J. Phys. Chem. Lett.* **2021**, *12*, 157−164.
(68) Frandsen, B. A.; Nickerson, S. D.; Clark, A. D.; Solano, A.; Baral, R.; Williams, J.; Neuefeind, J.; Memmott, M. The structure of molten FLiNaK. *J. Nucl. Mater.* **2020**, *537*, 152219.
(69) Li, Q.-J.; Sprouster, D.; Zheng, G.; Neuefeind, J. C.; Braatz, A. D.; Mcfarlane, J.; Olds, D.; Lam, S.; Li, J.; Khaykovich, B. Complex Structure of Molten NaCl-CrCl3 Salt: Cr-Cl Octahedral Network and Intermediate-Range Order. *ACS Applied Energy Materials* **2021**, *4*, 3044.
(70) Zachariasen, W. H. The atomic arrangement in glass. *J. Am. Chem. Soc.* **1932**, *54*, 3841−3851.
(71) Rosenhain, W. The structure and constitution of glass. *J. Soc. Glass Technol. Trans.* **1927**, *11*, 77.
(72) Whitman, M. J.; Stockton, D. L. *Boiling rubidium as a reactor coolant. Preparation of rubidium metal, physical and thermodynamic properties, and compatibility with INCONEL*; Oak Ridge School of Reactor Technology, 1954.
(73) Trauger, D. *Some major fuel-irradiation test facilities of the oak ridge national laboratory*;Oak Ridge National Laboratory, 1964.
(74) Briggs, R. B. *Molten-salt reactor program semiannual progress report*; Oak Ridge National Laboratory, 1964.
(75) Haubenreich, P. N.; Engel, J. R. Experience with the molten-salt experiment. *Nucl. Appl. Technol.* **1970**, *8*, 118−136.
(76) Sabharwall, P.; Aufiero, M.; Fratoni, M. In *Advances of Computational Fluid Dynamics in Nuclear Reactor Design and Safety Assessment*; Joshi, J. B., Nayak, A. K., Eds.; Woodhead Publishing Series in Energy; Woodhead Publishing, 2019; pp 801 − 834.
(77) Bradwell, D. J.; Kim, H.; Sirk, A. H. C.; Sadoway, D. R. Magnesium-antimony liquid metal battery for stationary energy storage. *J. Am. Chem. Soc.* **2012**, *134*, 1895−1897.
(78) Wagner, L. In *Future Energy*, 2nd ed.; Letcher, T. M., Ed.; Elsevier: Boston, 2014; pp 613 − 631.
(79) Bauer, T.; Pfleger, N.; Laing, D.; Steinmann, W.-D.; Eck, M.; Kaesche, S. In *Molten Salts Chemistry*; Lantelme, F., Groult, H., Eds.; Elsevier: Oxford, 2013; pp 415 − 438.
(80) Ellis, B. L.; Nazar, L. F. Sodium and sodium-ion energy storage batteries. *Curr. Opin. Solid State Mater. Sci.* **2012**, *16*, 168−177.
(81) Slater, M. D.; Kim, D.; Lee, E.; Johnson, C. S. Sodium-ion batteries. *Adv. Funct. Mater.* **2013**, *23*, 947−958.
(82) Spatocco, B. L.; Ouchi, T.; Lambotte, G.; Burke, P. J.; Sadoway, D. R. Low-temperature molten salt electrolytes for membrane-free sodium metal batteries. *J. Electrochem. Soc.* **2015**, *162*, A2729−A2736.
(83) Kim, S.-W.; Lee, J. K.; Ryu, D.; Jeon, M. K.; Hong, S.-S.; Heo, D. H.; Choi, E.-Y. Residual salt separation technique using centrifugal force for pyroprocessing. *Nucl. Eng. Technol.* **2018**, *50*, 1184−1189.
(84) Sharma, S.; Emerson, M. S.; Wu, F.; Wang, H.; Maginn, E. J.; Margulis, C. J. SEM-Drude model for the accurate and efficient simulation of $MgCl_2$−KCl mixtures in the condensed phase. *J. Phys. Chem. A* **2020**, *124*, 7832−7842.
(85) Liang, W.; Lu, G.; Yu, J. Machine-Learning-Driven Simulations on Microstructure and Thermophysical Properties of MgCl2−KCl Eutectic. *ACS Appl. Mater. Interfaces* **2021**, *13*, 4034−4042.
(86) Liang, W.; Lu, G.; Yu, J. Theoretical prediction on the local structure and transport properties of molten alkali chlorides by deep potentials. *J. Mater. Sci. Technol.* **2021**, *75*, 78−85.
(87) Tovey, S.; Narayanan Krishnamoorthy, A.; Sivaraman, G.; Guo, J.; Benmore, C.; Heuer, A.; Holm, C. DFT Accurate Interatomic Potential for Molten NaCl from Machine Learning. *J. Phys. Chem. C* **2020**, *124*, 25760−25768.
(88) Sivaraman, G.; Guo, J.; Ward, L.; Hoyt, N.; Williamson, M.; Foster, I.; Benmore, C.; Jackson, N. Automated Development of Molten Salt Machine Learning Potentials: Application to LiCl. *ChemRxiv* **2021**, DOI: 10.26434/chemrxiv.14226833.v1.
(89) Pan, G.; Chen, P.; Yan, H.; Lu, Y. A DFT accurate machine learning description of molten ZnCl2 and its mixtures: 1. Potential development and properties prediction of molten ZnCl2. *Comput. Mater. Sci.* **2020**, *185*, 109955.
(90) Li, Q.-J.; Küçükbenli, E.; Lam, S.; Khaykovich, B.; Kaxiras, E.; Li, J. Development of robust neural-network interatomic potential for molten salt. *Cell Rep. Physical Science* **2021**, *2*, 100359.
(91) Janz, G. J. Thermodynamic and transport properties of molten salts: Correlation equations for critically evaluated density, surface tension, electrical conductance, and viscosity data. *J. Phys. Chem. Ref. Data* **1988**, *17*.
(92) Qiao, G.; Lasfargues, M.; Alexiadis, A.; Ding, Y. Simulation and experimental study of the specific heat capacity of molten salt based nanofluids. *Appl. Therm. Eng.* **2017**, *111*, 1517−1522.
(93) Okamoto, Y.; Kobayashi, F.; Ogawa, T. Structure and dynamic properties of molten uranium trichloride. *J. Alloys Compd.* **1998**, *271*−*273*, 355−358.

https://doi.org/10.1021/acs.jpcb.1c01065
J. Phys. Chem. B 2021, 125, 6359−6372

(94) Okamoto, Y.; Madden, P.; Minato, K. X-ray diffraction and molecular dynamics simulation studies of molten uranium chloride. *J. Nucl. Mater.* **2005**, *344*, 109−114.
(95) Roy, S.; Wu, F.; Wang, H.; Ivanov, A. S.; Sharma, S.; Halstenberg, P.; Gill, S. K.; Milinda Abeykoon, A. M.; Kwon, G.; Topsakal, M.; et al. Structure and dynamics of the molten alkali-chloride salts from an X-ray, simulation, and rate theory perspective. *Phys. Chem. Chem. Phys.* **2020**, *22*, 22900−22917.
(96) Nunes, V. M. B.; Lourenço, M. J. V.; Santos, F. J. V.; Nieto de Castro, C. A. Importance of accurate data on viscosity and thermal conductivity in molten salts applications. *J. Chem. Eng. Data* **2003**, *48*, 446−450.
(97) Walden, P. *Bull. Acad. Imp. Sci. St. Petersburg* **1914**, *8*, 405−422.
(98) Hurley, F. H.; WIer, T. P. Electrodeposition of metals from fused quaternary ammonium salts. *J. Electrochem. Soc.* **1951**, *98*, 203.
(99) Welton, T. Ionic liquids: a brief history. *Biophys. Rev.* **2018**, *10*, 691−706.
(100) Fischer, H. E.; Barnes, A. C.; Salmon, P. S. Neutron and x-ray diffraction studies of liquids and glasses. *Rep. Prog. Phys.* **2006**, *69*, 233−299.
(101) Egami, T.; Billinge, S. *Underneath the Bragg Peaks*; Elsevier, 2012; Vol. *16*.
(102) Neuefeind, J. High energy XRD investigations of liquids. *J. Mol. Liq.* **2002**, *98*−*99*, 87−95.
(103) Benmore, C. J. A review of high-energy X-ray diffraction from glasses and liquids. *Int. Sch. Res. Notices* **2012**, *2012*, 852905.
(104) Kohara, S.; Itou, M.; Suzuya, K.; Inamura, Y.; Sakurai, Y.; Ohishi, Y.; Takata, M. Structural studies of disordered materials using high-energy x-ray diffraction from ambient to extreme conditions. *J. Phys.: Condens. Matter* **2007**, *19*, 506101.
(105) Keen, D. A. A comparison of various commonly used correlation functions for describing total scattering. *J. Appl. Crystallogr.* **2001**, *34*, 172−177.
(106) Halstenberg, P. W.; Maltsev, D.; Nguyen, D.; Kim, E.; Dai, S. Mechanochemical synthesis of high-purity anhydrous binary alkali and alkaline earth chloride mixtures. *Ind. Eng. Chem. Res.* **2020**, *59*, 19884−19889.
(107) Zarzycki, J. High-temperature X-ray diffraction study of molten salts. I. structure of fluorides LiF, NaF and KF in the liquid state. *J. Phys. Phys. Appl.* **1957**, *18*, 65−69.
(108) Bedrov, D.; Borodin, O.; Li, Z.; Smith, G. D. Influence of polarization on structural, thermodynamic, and dynamic properties of ionic liquids obtained from molecular dynamics simulations. *J. Phys. Chem. B* **2010**, *114*, 4984−4997.
(109) Fillion, J. J.; Brennecke, J. F. Viscosity of ionic liquid-ionic liquid mixtures. *J. Chem. Eng. Data* **2017**, *62*, 1884−1901.
(110) Bandrés, I.; Alcalde, R.; Lafuente, C.; Atilhan, M.; Aparicio, S. On the viscosity of pyridinium based ionic liquids: An experimental and computational study. *J. Phys. Chem. B* **2011**, *115*, 12499−12513.
(111) Murgulescu, I. G.; Zuca, S. Über die innere Reibung einiger einfacher, geschmolzener Salze. *Z. Phys. Chem.* **1962**, *218O*, 218O.
(112) Janz, G. J.; Tomkins, R. P. T.; Allen, C. B.; Downey, J. R.; Garner, G. L.; Krebs, U.; Singer, S. K. Molten salts: volume 4, part 2, chlorides and mixtures-electrical conductance, density, viscosity, and surface tension data. *J. Phys. Chem. Ref. Data* **1975**, *4*, 871−1178.
(113) Zhang, Y.; Otani, A.; Maginn, E. J. Reliable viscosity calculation from equilibrium molecular dynamics simulations: A time decomposition method. *J. Chem. Theory Comput.* **2015**, *11*, 3537−3546.
(114) Amith, W. D.; Araque, J. C.; Margulis, C. J. A pictorial view of viscosity in ionic liquids and the link to nanostructural heterogeneity. *J. Phys. Chem. Lett.* **2020**, *11*, 2062−2066.
(115) Goloviznina, K.; Canongia Lopes, J. N.; Costa Gomes, M.; Pádua, A. A. H. Transferable, polarizable force field for ionic liquids. *J. Chem. Theory Comput.* **2019**, *15*, 5858−5871.
(116) Kashyap, H. K.; Hettige, J. J.; Annapureddy, H. V. R.; Margulis, C. J. SAXS anti-peaks reveal the length-scales of dual positive−negative and polar−apolar ordering in room-temperature ionic liquids. *Chem. Commun.* **2012**, *48*, 5103−5105.
(117) Annapureddy, H. V. R.; Kashyap, H. K.; Biase, P. M. D.; Margulis, C. J. What is the origin of the prepeak in the x-ray scattering of imidazolium-based room-temperature ionic liquids? *J. Phys. Chem. B* **2010**, *114*, 16838−16846.
(118) Kashyap, H. K.; Margulis, C. J. (Keynote) Theoretical deconstruction of the x-ray structure function exposes polarity alternations in room temperature ionic liquids. *ECS Trans.* **2013**, *50*, 301−307.
(119) Araque, J. C.; Hettige, J. J.; Margulis, C. J. Modern room temperature ionic liquids, a simple guide to understanding their structure and how it may relate to dynamics. *J. Phys. Chem. B* **2015**, *119*, 12727−12740.
(120) Kashyap, H. K.; Santos, C. S.; Annapureddy, H. V. R.; Murthy, N. S.; Margulis, C. J.; Castner, E. W., Jr. Temperature-dependent structure of ionic liquids: X-ray scattering and simulations. *Faraday Discuss.* **2012**, *154*, 133−143.
(121) Hettige, J. J.; Kashyap, H. K.; Annapureddy, H. V. R.; Margulis, C. J. Anions, the reporters of structure in ionic liquids. *J. Phys. Chem. Lett.* **2013**, *4*, 105−110.
(122) Hettige, J. J.; Araque, J. C.; Margulis, C. J. Bicontinuity and multiple length scale ordering in triphilic hydrogen-bonding ionic liquids. *J. Phys. Chem. B* **2014**, *118*, 12706−12716.
(123) Hettige, J. J.; Araque, J. C.; Kashyap, H. K.; Margulis, C. J. Communication: Nanoscale structure of tetradecyltrihexylphosphonium based ionic liquids. *J. Chem. Phys.* **2016**, *144*, 121102.
(124) Kashyap, H. K.; Santos, C. S.; Daly, R. P.; Hettige, J. J.; Murthy, N. S.; Shirota, H.; Castner, E. W., Jr.; Margulis, C. J. How does the ionic liquid organizational landscape change when nonpolar cationic alkyl groups are replaced by polar isoelectronic diethers? *J. Phys. Chem. B* **2013**, *117*, 1130−1135.
(125) Kashyap, H. K.; Santos, C. S.; Murthy, N. S.; Hettige, J. J.; Kerr, K.; Ramati, S.; Gwon, J.; Gohdo, M.; Lall-Ramnarine, S. I.; Wishart, J. F.; et al. Structure of 1-alkyl-1-methylpyrrolidinium bis(trifluoromethylsulfonyl)amide ionic liquids with linear, branched, and cyclic alkyl groups. *J. Phys. Chem. B* **2013**, *117*, 15328−15337.
(126) Zhao, M.; Wu, B.; Lall-Ramnarine, S. I.; Ramdihal, J. D.; Papacostas, K. A.; Fernandez, E. D.; Sumner, R. A.; Margulis, C. J.; Wishart, J. F.; Castner, E. W. Structural analysis of ionic liquids with symmetric and asymmetric fluorinated anions. *J. Chem. Phys.* **2019**, *151*, 074504.
(127) Bradley, A. E.; Hardacre, C.; Holbrey, J. D.; Johnston, S.; McMath, S. E. J.; Nieuwenhuyzen, M. Small-Angle X-ray Scattering Studies of Liquid Crystalline 1-Alkyl-3-methylimidazolium Salts. *Chem. Mater.* **2002**, *14*, 629−635.
(128) Urahata, S. M.; Ribeiro, M. C. C. Structure of ionic liquids of 1-alkyl-3-methylimidazolium cations: A systematic computer simulation study. *J. Chem. Phys.* **2004**, *120*, 1855−1863.
(129) Wang, Y.; Voth, G. A. Tail aggregation and domain diffusion in ionic liquids. *J. Phys. Chem. B* **2006**, *110*, 18601−18608.
(130) Bhargava, B. L.; Devane, R.; Klein, M. L.; Balasubramanian, S. Nanoscale organization in room temperature ionic liquids: a coarse grained molecular dynamics simulation study. *Soft Matter* **2007**, *3*, 1395−1400.
(131) Canongia Lopes, J. N. A.; Pádua, A. A. H. Nanostructural Organization in Ionic Liquids. *J. Phys. Chem. B* **2006**, *110*, 3330−3335.
(132) Castner, E. W.; Wishart, J. F. Spotlight on ionic liquids. *J. Chem. Phys.* **2010**, *132*, 120901.
(133) Russina, O.; Triolo, A.; Gontrani, L.; Caminiti, R.; Xiao, D.; Jr, L. G. H.; Bartsch, R. A.; Quitevis, E. L.; Pleckhova, N.; Seddon, K. R. Morphology and intermolecular dynamics of 1-alkyl-3-methylimidazolium bis{(trifluoromethane)sulfonyl}amide ionic liquids: structural and dynamic evidence of nanoscale segregation. *J. Phys.: Condens. Matter* **2009**, *21*, 424121.
(134) Triolo, A.; Russina, O.; Bleif, H.-J.; Di Cola, E. Nanoscale segregation in room temperature ionic liquids. *J. Phys. Chem. B* **2007**, *111*, 4641−4644.
(135) Salanne, M.; Siqueira, L. J. A.; Seitsonen, A. P.; Madden, P. A.; Kirchner, B. From molten salts to room temperature ionic liquids:

https://doi.org/10.1021/acs.jpcb.1c01065
J. Phys. Chem. B 2021, 125, 6359−6372

Simulation studies on chloroaluminate systems. *Faraday Discuss.* **2012**, *154*, 171−188.
(136) Schröder, C. Comparing reduced partial charge models with polarizable simulations of ionic liquids. *Phys. Chem. Chem. Phys.* **2012**, *14*, 3089−3102.
(137) Schröder, C.; Steinhauser, O. Simulating polarizable molecular ionic liquids with Drude oscillators. *J. Chem. Phys.* **2010**, *133*, 154511.
(138) Pádua, A. A. H. Resolving dispersion and induction components for polarisable molecular simulations of ionic liquids. *J. Chem. Phys.* **2017**, *146*, 204501.
(139) Heid, E.; Boresch, S.; Schröder, C. Polarizable molecular dynamics simulations of ionic liquids: Influence of temperature control. *J. Chem. Phys.* **2020**, *152*, 094105.
(140) McDaniel, J. G.; Schmidt, J. Physically-motivated force fields from symmetry-adapted perturbation theory. *J. Phys. Chem. A* **2013**, *117*, 2053−2066.
(141) McDaniel, J. G.; Son, C. Y.; Yethiraj, A. Ab Initio force fields for organic anions: Properties of [BMIM][TFSI], [BMIM][FSI], and [BMIM][OTf] ionic liquids. *J. Phys. Chem. B* **2018**, *122*, 4101−4114.
(142) McDaniel, J. G.; Yethiraj, A. Understanding the properties of ionic liquids: Electrostatics, structure factors, and their sum rules. *J. Phys. Chem. B* **2019**, *123*, 3499−3512.
(143) Salmon, P. S. The structure of molten and glassy 2:1 binary systems: An approach using the Bhatia-Thornton formalism. *Proc. R. Soc. London A* **1992**, *437*, 591−606.
(144) Hardacre, C.; Holbrey, J. D.; Mullan, C. L.; Youngs, T. G. A.; Bowron, D. T. Small angle neutron scattering from 1-alkyl-3-methylimidazolium hexafluorophosphate ionic liquids ($[C_n mim][PF_6]$, n = 4, 6, and 8). *J. Chem. Phys.* **2010**, *133*, 074510.
(145) Chabrier, G.; Senatore, G.; Tosi, M. *Ionic structure of solutions of alkali metals and molten salts*; International Atomic Energy Agency (IAEA), 1982.
(146) Adya, A. K.; Takagi, R.; Gaune-Escard, M. Unravelling the Internal Complexities of Molten Salts. *Z. Naturforsch., A: Phys. Sci.* **1998**, *53*, 1037−1048.
(147) Araque, J. C.; Hettige, J. J.; Margulis, C. J. Ionic liquids-conventional solvent mixtures, structurally different but dynamically similar. *J. Chem. Phys.* **2015**, *143*, 134505.
(148) Triolo, A.; Russina, O.; Fazio, B.; Triolo, R.; Cola, E. D. Morphology of 1-alkyl-3-methylimidazolium hexafluorophosphate room temperature ionic liquids. *Chem. Phys. Lett.* **2008**, *457*, 362−365.
(149) Chiappe, C. Nanostructural Organization of Ionic Liquids: Theoretical and Experimental Evidences of the Presence of Well Defined Local Structures in Ionic Liquids. *Monatsh. Chem.* **2007**, *138*, 1035−1043.
(150) Xiao, D.; Rajian, J. R.; Li, S.; Bartsch, R. A.; Quitevis, E. L. Additivity in the Optical Kerr Effect Spectra of Binary Ionic Liquid Mixtures: Implications for Nanostructural Organization. *J. Phys. Chem. B* **2006**, *110*, 16174−16178.
(151) Yan, T.; et al. Molecular dynamics simulation of ionic liquids: The effect of electronic polarizability. *J. Phys. Chem. B* **2004**, *108*, 11877−11881.
(152) Del Pópolo, M. G.; Voth, G. A. On the structure and dynamics of ionic liquids. *J. Phys. Chem. B* **2004**, *108*, 1744−1752.
(153) Wang, Y.; Jiang, W.; Yan, T.; Voth, G. A. Understanding ionic liquids through atomistic and coarse-grained molecular dynamics simulations. *Acc. Chem. Res.* **2007**, *40*, 1193−1199.
(154) Kirchner, B.; Hollóczki, O.; Canongia Lopes, J. N.; Pádua, A. A. H. Multiresolution calculation of ionic liquids. *Wires Comput. Mol. Sci.* **2015**, *5*, 202−214.
(155) Canongia Lopes, J. N.; Pádua, A. A. CLP: A generic and systematic force field for ionic liquids modeling. *Theor. Chem. Acc.* **2012**, *131*, 131.
(156) Pádua, A. A.; Costa Gomes, M. F.; Canongia Lopes, J. N. Molecular solutes in ionic liquids. *Acc. Chem. Res.* **2007**, *40*, 1087−1096.
(157) Canongia Lopes, J. N.; Costa Gomes, M. F.; Pádua, A. A. Nonpolar, polar, and associating solutes in ionic liquids. *J. Phys. Chem. B* **2006**, *110*, 16816−16818.
(158) Canongia Lopes, J. N.; Pádua, A. A. Nanostructural organization in ionic liquids. *J. Phys. Chem. B* **2006**, *110*, 3330−3335.
(159) Deetlefs, M.; Hardacre, C.; Nieuwenhuyzen, M.; Padua, A. A.; Sheppard, O.; Soper, A. K. Liquid structure of the ionic liquid 1,3-dimethylimidazolium bis(trifluoromethyl)sulfonylamide. *J. Phys. Chem. B* **2006**, *110*, 12055−12061.
(160) Hardacre, C.; Holbrey, J. D.; McMath, S. E.; Bowron, D. T.; Soper, A. K. Structure of molten 1,3-dimethylimidazolium chloride using neutron diffraction. *J. Chem. Phys.* **2003**, *118*, 273−278.
(161) Dupont, J. From molten salts to ionic liquids: A "nano" journey. *Acc. Chem. Res.* **2011**, *44*, 1223−1231.
(162) Cabry, C. P.; D'Andrea, L.; Shimizu, K.; Grillo, I.; Li, P.; Rogers, S.; Bruce, D. W.; Canongia Lopes, J. N.; Slattery, J. M. Exploring the bulk-phase structure of ionic liquid mixtures using small-angle neutron scattering. *Faraday Discuss.* **2018**, *206*, 265−289.
(163) Bruce, D. W.; Cabry, C. P.; Lopes, J. N.; Costen, M. L.; D'Andrea, L.; Grillo, I.; Marshall, B. C.; McKendrick, K. G.; Minton, T. K.; Purcell, S. M.; et al. Nanosegregation and Structuring in the Bulk and at the Surface of Ionic-Liquid Mixtures. *J. Phys. Chem. B* **2017**, *121*, 6002−6020.
(164) Mackoy, T.; Mauro, N. A.; Wheeler, R. A. Temperature dependence of static structure factor peak intensities for a pyrrolidinium-based ionic liquid. *J. Phys. Chem. B* **2019**, *123*, 1672−1678.
(165) Celso, F. L.; Appetecchi, G. B.; Simonetti, E.; Keiderling, U.; Gontrani, L.; Triolo, A.; Russina, O. Mesoscopic structural organization in fluorinated pyrrolidinium-based room temperature ionic liquids. *J. Mol. Liq.* **2019**, *289*, 111110.
(166) Wu, B.; Kuroda, K.; Takahashi, K.; Castner, E. W. Structural analysis of zwitterionic liquids vs. homologous ionic liquids. *J. Chem. Phys.* **2018**, *148*, 193807.
(167) Jiang, H. J.; Atkin, R.; Warr, G. G. Nanostructured ionic liquids and their solutions: Recent advances and emerging challenges. *Current Opinion in Green and Sustainable Chemistry* **2018**, *12*, 27−32.
(168) Russina, O.; Triolo, A. New experimental evidence supporting the mesoscopic segregation model in room temperature ionic liquids. *Faraday Discuss.* **2012**, *154*, 97−109.
(169) Paredes, X.; Fernández, J.; Pádua, A. A.; Malfreyt, P.; Malberg, F.; Kirchner, B.; Pensado, A. S. Bulk and liquid-vapor interface of pyrrolidinium-based ionic liquids: A molecular simulation study. *J. Phys. Chem. B* **2014**, *118*, 731−742.
(170) Lo Celso, F.; Appetecchi, G. B.; Jafta, C. J.; Gontrani, L.; Canongia Lopes, J. N.; Triolo, A.; Russina, O. Nanoscale organization in the fluorinated room temperature ionic liquid: Tetraethyl ammonium (trifluoromethanesulfonyl)(nonafluorobutylsulfonyl)-imide. *J. Chem. Phys.* **2018**, *148*, 193816.
(171) Lo Celso, F.; Yoshida, Y.; Lombardo, R.; Jafta, C.; Gontrani, L.; Triolo, A.; Russina, O. Mesoscopic structural organization in fluorinated room temperature ionic liquids. *C. R. Chim.* **2018**, *21*, 757−770.
(172) Montes-Campos, H.; Otero-Mato, J. M.; Méndez-Morales, T.; López-Lago, E.; Russina, O.; Cabeza, O.; Gallego, L. J.; Varela, L. M. Nanostructured solvation in mixtures of protic ionic liquids and long-chained alcohols. *J. Chem. Phys.* **2017**, *146*, 124503.
(173) Russina, O.; Caminiti, R.; Méndez-Morales, T.; Carrete, J.; Cabeza, O.; Gallego, L. J.; Varela, L. M.; Triolo, A. How does lithium nitrate dissolve in a protic ionic liquid? *J. Mol. Liq.* **2015**, *205*, 16−21.
(174) Hayes, R.; Imberti, S.; Warr, G. G.; Atkin, R. How water dissolves in protic ionic liquids. *Angew. Chem., Int. Ed.* **2012**, *51*, 7468−7471.
(175) Russina, O.; Lo Celso, F.; Plechkova, N. V.; Triolo, A. Emerging Evidences of Mesoscopic-Scale Complexity in Neat Ionic Liquids and Their Mixtures. *J. Phys. Chem. Lett.* **2017**, *8*, 1197−1204.
(176) Russina, O.; Sferrazza, A.; Caminiti, R.; Triolo, A. Amphiphile meets amphiphile: Beyond the polar-apolar dualism in ionic liquid/alcohol mixtures. *J. Phys. Chem. Lett.* **2014**, *5*, 1738−1742.

https://doi.org/10.1021/acs.jpcb.1c01065
J. Phys. Chem. B 2021, 125, 6359−6372

(177) Mé Ndez-Morales, T.; Carrete, J. S.; Rodrí Guez, A. O.; Scar Cabeza, J. R.; Gallego, L. J.; Russina, O.; Varela, L. M. Nanostructure of mixtures of protic ionic liquids and lithium salts: effect of alkyl chain length. *Phys. Chem. Chem. Phys.* **2015**, *17*, 5298.
(178) Zheng, W.; Mohammed, A.; Hines, L. G.; Xiao, D.; Martinez, O. J.; Bartsch, R. A.; Simon, S. L.; Russina, O.; Triolo, A.; Quitevis, E. L. Effect of cation symmetry on the morphology and physicochemical properties of imidazolium ionic liquids. *J. Phys. Chem. B* **2011**, *115*, 6572−6584.
(179) Russina, O.; Celso, F. L.; Triolo, A. Pressure-responsive mesoscopic structures in room temperature ionic liquids. *Phys. Chem. Chem. Phys.* **2015**, *17*, 29496−29500.
(180) Triolo, A.; Russina, O.; Fazio, B.; Appetecchi, G. B.; Carewska, M.; Passerini, S. Nanoscale organization in piperidinium-based room temperature ionic liquids. *J. Chem. Phys.* **2009**, *130*, 164521.
(181) Russina, O.; Triolo, A.; Gontrani, L.; Caminiti, R. Mesoscopic structural heterogeneities in room-temperature ionic liquids. *J. Phys. Chem. Lett.* **2012**, *3*, 27−33.
(182) Hayes, R.; Warr, G. G.; Atkin, R. Structure and nanostructure in ionic liquids. *Chem. Rev.* **2015**, *115*, 6357−6426.
(183) Triolo, A.; Russina, O.; Bleif, H.-J.; Di Cola, E. Nanoscale Segregation in Room Temperature Ionic Liquids. *J. Phys. Chem. B* **2007**, *111*, 4641−4644.
(184) Xiao, D.; Hines, L. G.; Li, S.; Bartsch, R. A.; Quitevis, E. L.; Russina, O.; Triolo, A. Effect of Cation Symmetry and Alkyl Chain Length on the Structure and Intermolecular Dynamics of 1,3-Dialkylimidazolium Bis(trifluoromethanesulfonyl)amide Ionic Liquids. *J. Phys. Chem. B* **2009**, *113*, 6426−6433.
(185) Xiao, D.; Rajian, J. R.; Cady, A.; Li, S.; Bartsch, R. A.; Quitevis, E. L. Nanostructural Organization and Anion Effects on the Temperature Dependence of the Optical Kerr Effect Spectra of Ionic Liquids. *J. Phys. Chem. B* **2007**, *111*, 4669−4677.
(186) Bardak, F.; Xiao, D.; Hines, L. G., Jr.; Son, P.; Bartsch, R. A.; Quitevis, E. L.; Yang, P.; Voth, G. A. Nanostructural Organization in Acetonitrile/Ionic Liquid Mixtures: Molecular Dynamics Simulations and Optical Kerr Effect Spectroscopy. *ChemPhysChem* **2012**, *13*, 1687−1700.
(187) Wilson, M. Structure and dynamics in network-forming materials. *J. Phys.: Condens. Matter* **2016**, *28*, 503001.
(188) Hettige, J. J.; Kashyap, H. K.; Margulis, C. J. Communication: Anomalous temperature dependence of the intermediate range order in phosphonium ionic liquids. *J. Chem. Phys.* **2014**, *140*, 111102.
(189) Roy, S.; Brehm, M.; Sharma, S.; Wu, F.; Maltsev, D. S.; Halstenberg, P.; Gallington, L. C.; Mahurin, S. M.; Dai, S.; Ivanov, A. S.; Margulis, C. J.; Bryantsev, V. S. Unraveling Local Structure of Molten Salts via X-ray Scattering, Raman Spectroscopy, and *Ab Initio* Molecular Dynamics. *J. Phys. Chem. B* **2021**, DOI: 10.1021/acs.jpcb.1c03786.

https://doi.org/10.1021/acs.jpcb.1c01065
J. Phys. Chem. B 2021, 125, 6359−6372